Alamethicin Helices in a Bilayer and in Solution: Molecular Dynamics Simulations

D. Peter Tieleman,* Mark S. P. Sansom,# and Herman J. C. Berendsen*
*BIOSON Research Institute and Department of Biophysical Chemistry, University of Groningen, 9747 AG Groningen, The Netherlands, and #Laboratory of Molecular Biophysics, Department of Biochemistry, University of Oxford, Oxford OX1 3QU, England

ABSTRACT Alamethicin is an α-helical channel-forming peptide, which inserts into lipid bilayers in a voltage-dependent, asymmetrical fashion. Nanosecond molecular dynamics simulations have been used to compare alamethicin conformation and dynamics in three different environments: 1) in water; 2) in methanol; and 3) inserted into a lipid (palmitoyl-oleoyl-phosphatidylcholine) bilayer to form a transmembrane helix. In the bilayer and in methanol, there was little change (Cα RMSD $\approx$ 0.2 nm over 2 ns and 1 ns) from the initial helical conformation of the peptide. In water there were substantial changes (Cα RMSD $\approx$ 0.4 nm over 1 ns), especially in the C-terminal segment of the peptide, which lost its α-helical conformation. In the bilayer and in methanol, the alamethicin molecule underwent hinge-bending motion about its central Gly-X-X-Pro sequence motif. Analysis of H-bonding interactions revealed that the polar C-terminal side chains of alamethicin provided an "anchor" to the bilayer/water interface via formation of multiple H-bonds that persisted throughout the simulation. This explains why the preferred mode of helix insertion into the bilayer is N-terminal, which is believed to underlie the asymmetry of voltage activation of alamethicin channels.

INTRODUCTION

Integral membrane proteins make up ~25% of all proteins (Boyd et al., 1998; Wallin and von Heijne, 1998), and yet we know relatively little, compared with globular proteins, about their structures and the factors that stabilize their structures. From sequence analysis it appears that the majority of membrane proteins are composed of transmembrane (TM) α-helices. It is therefore of interest to understand the structure and dynamics of TM helices in a lipid bilayer environment. One way in which this may be addressed is to study relatively simple peptides that form TM helices and thus may be considered models of these components of more complex membrane proteins. In this way it is possible to elucidate the physicochemical principles of TM helix stability. Naturally occurring α-helical peptides that interact with lipid bilayers are also of interest per se, as they frequently exhibit antimicrobial and/or cytolytic properties (Gazit et al., 1996; La Rocca et al., manuscript submitted for publication; Sansom, 1991). There are also a number of TM helices that have emerged from de novo synthetic studies (Åkerfeldt et al., 1993; Lear et al., 1988, 1994).

The peptaibols are a family of fungal peptides that form ion channels in lipid bilayers (Cafiso, 1994; Sansom, 1993; Woolley and Wallace, 1992). The best known member of this family is the channel-forming peptide alamethicin (Alm). Alm exists as two major variants, the R_f30 form,

Ac-Aib-Pro-Aib-Ala-Aib-Ala-Gln^{7}-Aib-Val-Aib-

Gly-Leu-Aib-Pro^{14}-Val-Aib-Aib-Glu^{18}-Gln-Phol

and the R_f50 form in which Glu^{18} is replaced by Gln. The sequence of Alm contains a preponderance of a helicogenic amino acid, namely α-amino isobutyric acid (Aib). There is a proline close to the center of the molecule at position 14 and a C-terminal phenylalaninol residue (Phol; i.e., the terminal -CO_2H is replaced by -CH_2OH). The structure of Alm in a nonaqueous environment has been solved both by x-ray diffraction (Fox and Richards, 1982) and by NMR (Esposito et al., 1987; Franklin et al., 1994). The two structures are strikingly similar. The high content of Aib ensures that Alm adopts a largely α-helical conformation. The presence of Pro^{14} induces a central kink in the helix. NMR amide exchange data demonstrate that the largely α-helical conformation of Alm when dissolved in methanol (MeOH) (Dempsey, 1995) is retained when it interacts with lipid bilayers (Dempsey and Handcock, 1996). Comparison of amide exchange data with MD simulations suggests that Alm in MeOH undergoes hinge-bending motion about the central proline-induced kink (Gibbs et al., 1997).

Channel formation by Alm is voltage dependent. The resultant channels switch rapidly (on a ~10-ms time scale) between multiple conductance levels. An early event on the pathway to channel formation is voltage-dependent insertion of an Alm helix into the lipid bilayer (see reviews by Cafiso, 1994; Sansom, 1993). Many studies of the interactions of Alm with bilayers have focused on the orientation of Alm helices relative to the lipid bilayer. Early studies using CD spectroscopy on oriented multibilayers (Vogel, 1987) suggested that the orientation of Alm helices relative to the bilayer normal was sensitive to the percentage hydra-

Received for publication 16 June 1998 and in final form 17 September 1998.

Address reprint requests to Dr. Mark S. P. Sansom, Laboratory of Molecular Biophysics, The Rex Richards Building, University of Oxford, South Parks Road, Oxford OX1 3QU, England. Tel.: +44-1865-275371; Fax: +44-1865-275182; E-mail: mark@biop.ox.ac.uk.

0006-3495/99/01/40/10 $2.00

tion and the phase of the lipid. Huang and Wu (1991), also on the basis of CD studies, stressed the dependence of helix orientation on the peptide-to-lipid ratio, an increase in peptide favoring an inserted orientation over a surface-associated orientation. Studies using spin-labeled Alm and ESR (Barranger-Mathys and Cafiso, 1996) or solid-state NMR of ^{15}N-labeled Alm (North et al., 1995) also suggest that Alm helices may insert into lipid bilayers. Overall, the data suggest that Alm exists in a dynamic equilibrium between a surface-associated and a bilayer-inserted form. (However, as the surface-associated form is only seen at less than 100% hydration if lipids other than diphytanoyl PC are employed, there remains a degree of uncertainty over this conclusion.) A surface-associated Alm helix could, in principle, insert in either of two manners: 1) via the N-terminus crossing the bilayer or 2) via C-terminal insertion. The experimental evidence suggests that N-terminal insertion is favored over C-terminal insertion (Sansom, 1993). In particular, voltage activation of Alm channels, of which helix insertion is the first step, only occurs when the side of the membrane on which Alm is present (the *cis* face) experiences a positive voltage relative to the opposite (*trans*) face. The positive voltage repels the N-terminal component of the α-helical dipole of Alm, leading to its insertion into the membrane. If the *cis* face is made negative, even though the C-terminal end of the helix dipole is repelled, insertion does not occur. This suggests that some feature of the C-terminus of the Alm helix must act as an "anchor" at the bilayer surface, preventing C-terminal insertion.

One way in which peptide/bilayer interactions may be explored at atomic resolution is via molecular dynamics (MD) simulations. There have been a number of MD simulation studies of Alm: 1) studies in vacuo (Fraternali, 1990); 2) studies in MeOH (Gibbs et al., 1997; Sessions et al., 1998); and 3) studies using a simple mean field model of a lipid bilayer plus transbilayer voltage difference (Biggin et al., 1997). These simulations have yielded valuable information concerning the conformational dynamics of Alm. However, none of them have fully addressed the question of how an Alm helix behaves when inserted into a lipid bilayer. The past few years have seen considerable advances in MD simulations of lipid bilayers (see reviews by Jakobsson, 1997; Merz, 1997; Merz and Roux, 1996; Tieleman et al., 1997; Tobias et al., 1997). It is now quite feasible to use MD simulations to explore TM helices and their interactions with bilayers at atomic resolution. This has been done for a polyalanine model of a TM helix (Shen et al., 1997), for isolated helices from bacteriorhodopsin (Woolf, 1997), and for a simply designed TM helical peptide (Belohorcova et al., 1997). It is therefore timely to extend this approach to Alm.

In this paper we are concerned with the bilayer-inserted form of Alm. (The surface-associated form and the nature of the transition between associated and inserted forms will be the subjects of future publications.) However, Alm must exist in aqueous solution before binding to and inserting into bilayers. Furthermore, many spectroscopic and related studies (including MD simulations; see Gibbs et al., 1997) of Alm have been performed in MeOH. For the purposes of comparison, both with experimental data and between different simulation environments, we have performed MD simulations of 1 or 2 ns duration on Alm in water, in MeOH, and inserted into a palmitoyl-oleoyl-phosphatidylcholine (POPC) bilayer. We simulated the R_f30 (i.e., Glu^{18}) form of Alm. However, we recognize that the Glu^{18} residue may shift its pK_A and thus protonate when in an apolar environment. Thus, for the POPC-inserted helix, we have simulated Alm with residue Glu^{18} ionized (henceforth Alm$^-$) and with Glu^{18} protonated (henceforth AlmH). We explore the effect of environment on the conformational dynamics of Alm and attempt to explain the nature of the C-terminal "anchor" that favors N-terminal insertion of the Alm helix.

METHODS

Initial structure

The initial structure of Alm was generated by restrained MD simulations in vacuo and a simulated annealing protocol, as described by, e.g., Biggin et al. (1997). However, we note that previous studies (Biggin et al., 1997) have shown that the Alm model thus generated is very close in its backbone conformation to the x-ray structure (Fox and Richards, 1982). For example, the Cα RMSD between the three monomers in the asymmetrical unit of the x-ray structure is 0.074 nm, whereas the RMSD for the starting model used in this simulation versus the three x-ray structures is 0.088 nm.

Systems

Simulations were carried out for the following systems: 1) Alm$^-$ with 3467 water molecules plus one Na^+ ion (henceforth Alm/water), giving a total of 10,569 atoms in an initial box size of $4.9 \times 4.8 \times 4.9$ nm^3; 2) Alm$^-$ with 1682 MeOH molecules plus one Na^+ ion (henceforth Alm/MeOH), giving a total of 5157 atoms in an initial box of $4.9 \times 4.8 \times 4.9$ nm^3; 3) Alm$^-$ inserted in a bilayer of 127 POPC molecules plus one Na^+ ion and 3822 waters (henceforth Alm/POPC), giving a total of 18,238 atoms in a initial box of $6.2 \times 6.0 \times 7.6$ nm^3; and AlmH inserted in the same POPC bilayer, with the same number of waters but no Na^+ ion (henceforth AlmH/POPC).

For Alm/water and Alm/MeOH the initial system was generated by placing the Alm helix in a suitably sized box and then solvating. All solvent atoms that approached peptide atoms closer than the sum of their van der Waals radii were excluded. For Alm/POPC a fully equilibrated POPC bilayer of 128 lipid molecules was used. A short in vacuo MD simulation was performed in which a radial force was applied to exclude lipid atoms from a cylinder of radius 0.7 nm. The Alm monomer was placed in the resultant cylindrical "hole" in the lipid bilayer, such that the two ends of the helix were approximately coincident with the bilayer/water "interfaces," and such that the long axis of the helix was parallel to the bilayer normal (i.e., the z axis in our coordinate system). It was necessary to remove a single POPC molecule, the fatty acyl tails of which still overlapped with the peptide. This system was solvated with SPC water (at least 30 waters per lipid molecule) and energy minimized. For the Alm/POPC system, a single Na^+ ion was added, using a procedure that systematically positioned the ion instead of each water molecule in turn, eventually selecting the ion position with the lowest potential energy. After addition of the ion, the system was reminimized. The AlmH/POPC system was set up by taking the Alm/POPC system and protonating the Glu side chain, followed by energy minimization. A snapshot of the Alm/POPC system after minimization is shown in Fig. 1.

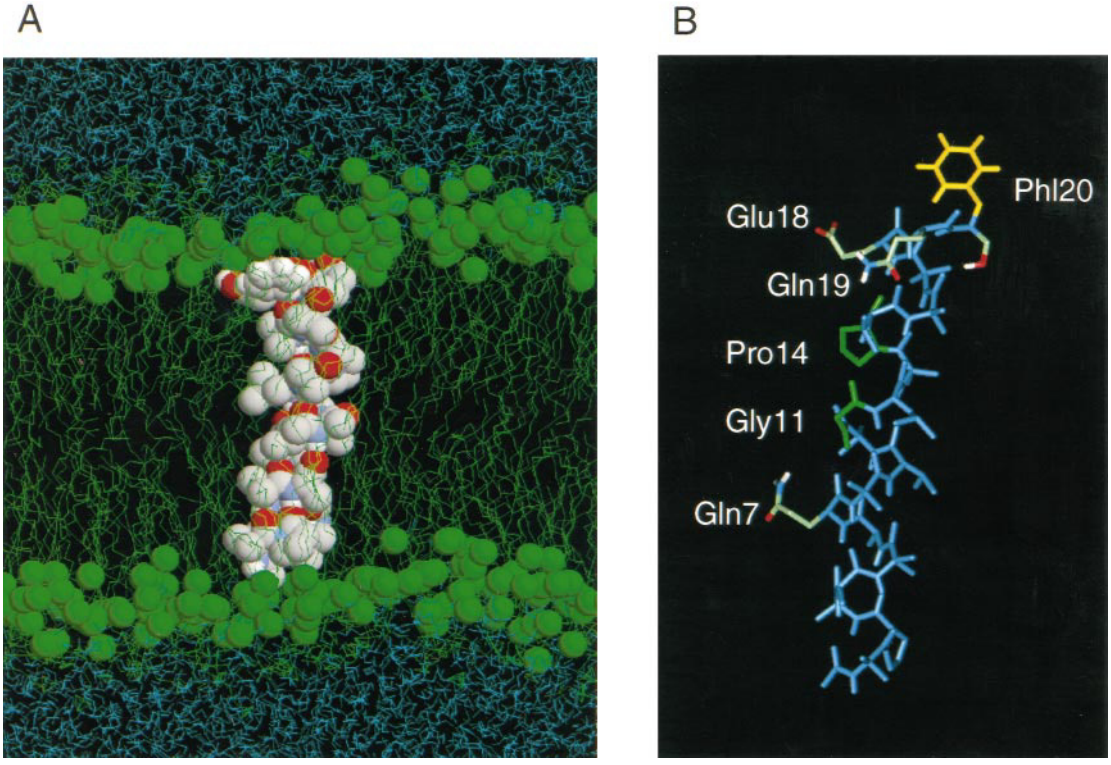

FIGURE 1 (*A*) Snapshot of the simulation system for an Alm monomer (*cpk colors*) inserted in a POPC bilayer (*green*) with water (*cyan*) on either side. The carbonyl atoms of the lipid headgroups and the Alm molecule are shown in space-filling format. (*B*) Diagram of an Alm monomer, highlighting polar side chains (Gln^{7}, Glu^{18}, and Gln^{19}, in *red/white/blue*), the region around the helix kink (Gly^{11}, Pro^{14}, in *green*), and the C-terminal amino alcohol (Phl^{20}, in *yellow*).

Dynamics simulations

Molecular dynamics simulations were run using GROMACS (Berendsen et al., 1995). A twin-range cutoff was used for longer range interactions: 1.0 nm for van der Waals interactions and 1.8 nm for electrostatic interactions. The time step was 2 fs, using SHAKE to constrain bond lengths. We used NPT conditions (i.e., constant number of particles, pressure, and temperature) in the simulation. A constant pressure of 1 bar in all three directions was used, with a coupling constant of $\tau_P = 1.0$ ps (Berendsen et al., 1984). This allows the bilayer/peptide area to adjust to its optimum value for the force field employed. The pros and cons of this approach have been discussed by, e.g., Tobias et al. (1997). Water, lipid, and protein were coupled separately to a temperature bath at 300 K, with a coupling constant $\tau_T = 0.1$ ps. The velocities of the atoms were not scaled during the simulation. Although the use of separate temperature baths for different components of the system may be considered unphysical, it is necessary to avoid temperature gradients, and the parameters used have been chosen empirically to minimize the known drawbacks of this procedure.

The lipid parameters were as in previous MD studies of lipid bilayers (Berger et al., 1997; Marrink et al., 1998). These lipid parameters give good reproduction of the experimental properties of a dipalmitoylphosphatidylcholine bilayer. The water model used was SPC (Hermans et al., 1984; van Gunsteren et al., 1996), which has been shown to behave well in lipid bilayer/water simulations (Tieleman and Berendsen, 1996).

Computational details

Simulations were carried out on a 10-processor, 195-MHz R10000 Origin 2000 and took ~8 days per processor per 1-ns simulation. Analysis was performed using facilities within GROMACS and with code written specifically for this project. Secondary structure analysis employed the DSSP algorithm (Kabsch and Sander, 1983). Essential dynamics and domain motion analysis (using DYNDOM) were performed as described by Hayward and Berendsen (1998). Structures were examined using Quanta (Biosym/MSI) and Rasmol, and diagrams were drawn using MolScript (Kraulis, 1991).

RESULTS

Cα RMSDs versus *t* for the different systems

The first two simulations, Alm/water and Alm/MeOH, were chosen to examine the stability of the Alm helix in aqueous solution and in nonaqueous (but isotropic) solution. The difference in the solvent has a marked effect on the progress of the simulations, as may be seen from examination of the Cα RMSDs versus time (Fig. 2 *A*). For Alm/water the RMSD rises almost continuously over the first ~350 ps, to a peak of ~0.4 nm. It then fluctuates on a 100-ps time scale between ~0.25 and 0.5 nm. Evidently, major changes in the conformation of Alm occur when the peptide is in water. This is in marked contrast to the Cα RMSD for Alm/MeOH, which rises to ~0.25 nm during the first 100 ps of the simulation and then fluctuates between ~0.1 and 0.28 nm, reaching a value of ~0.18 nm after 1 ns. This suggests that the Alm x-ray structure is largely maintained in MeOH, at least on the time scale sampled in these simulations. Thus, in isotropic solution, the Alm structure seems to require a nonaqueous solvent for stability. Note that the Alm was

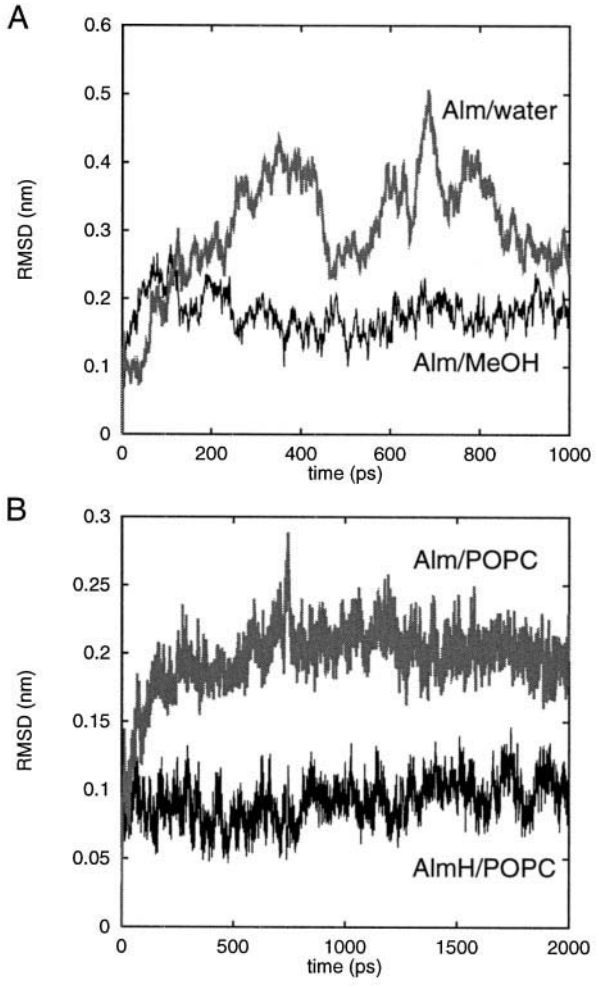

FIGURE 2 RMSDs versus time for the Cα atoms in each simulation. (*A*) Alm/water (*gray line*) and Alm/MeOH (*black line*). (*B*) Alm/POPC (*gray line*) and AlmH/POPC (*black line*).

crystallized from methanol/acetonitrile (Fox and Richards, 1982).

One may compare the Cα RMSDs from these simulations with those obtained for the same Alm molecule inserted in a POPC bilayer (Fig. 2 *B*). For Alm/POPC the RMSD rises over ~250 ps (i.e., possibly a little more slowly than in MeOH) to ~0.20 nm. It then fluctuates about that value for the remainder of the 2-ns simulation, showing no tendency to increase further. Thus the helical structure of Alm seems to be largely retained when it is inserted into a bilayer. A similar result is seen for AlmH/POPC, although the overall RMSD (from essentially the same starting conformation) is somewhat lower. This reflects a difference in the two simulations, with a small conformational change in the N-segment of the helix occurring in Alm/POPC at ~100 ps (see below). However, this is the only noticeable difference between the Alm/POPC and AlmH/POPC simulations. Thus the overall stability of the Alm helix seems to be about the same in a bilayer-inserted orientation as in solution in MeOH.

Fluctuations in structures

In addition to looking at the "drift" from the starting structure, it is valuable to compare the magnitudes of the structural fluctuations about the time-averaged structure (not the initial structure, in contrast to the RMSD, as discussed in the previous section) for each simulation. In Fig. 3 the Cα RMS fluctuations from the average are examined as a function of residue number. This confirms the similarity of the Alm/MeOH, Alm/POPC, and AlmH/POPC simulations and their difference from Alm/water. Thus, for Alm/MeOH, Alm/POPC, and AlmH/POPC the Cα RMSF versus residue plot is relatively flat. Other than for the terminal residues, the fluctuations are less than 0.1 nm, and for the central core they are nearly as low as 0.05 nm. There is no difference along the length of the helix, i.e., residues N-terminal to the proline-induced kink do not exhibit a lower RMSF than those in the C-terminal segment. The corresponding graph for Alm/water is markedly different. The overall magnitude of the RMSFs is higher, ranging from 0.15 to 0.2 nm. Furthermore, the RMSFs are lower for the N-terminal segment (particularly residues 1–7) of the molecule. The RMSFs are highest for those residues C-terminal to the proline (i.e., 14–20). Overall, the RMSFs confirm the picture of the Alm helix as stable in a hydrophobic environment, whether in isotropic solution or inserted into a bilayer, but less stable in an aqueous environment, where disordering of the C-terminal half of the molecule occurs. Furthermore, relative to their average structures, Alm/POPC and AlmH/POPC do not show any difference in the magnitudes of their fluctuations.

Hinge bending and the Pro-induced kink

There has been some discussion of the role of intrahelical prolines, such as that in Alm, in possible hinge-bending motions in transmembrane helices (Brandl and Deber, 1986;

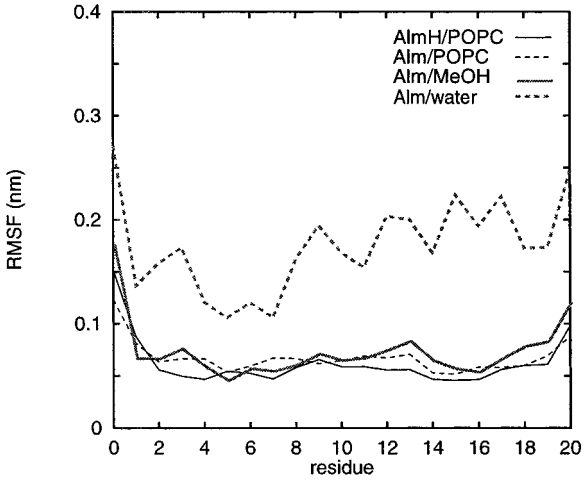

FIGURE 3 Residue-by-residue Cα RMS fluctuations around their average positions for Alm/water (*broken gray line*), Alm/MeOH (*solid gray line*), Alm/POPC (*broken black line*), and AlmH/POPC (*solid black line*).

Polinsky et al., 1992; Sankararamakrishnan and Vishveshwara, 1992; Sansom, 1992; von Heijne, 1991; Woolfson et al., 1991; Yun et al., 1992). It is therefore of interest to examine the role of motions around the proline-induced kink in Alm in different environments. One way of visualizing this, which has been employed in, for example, NMR studies of peptide helix conformations, is to superimpose snapshots of the peptide structure taken from the MD trajectory on, e.g., the N-terminal half (up to Gly^{11}) of the molecule (Fig. 4). It should be emphasized that this is simply a way of displaying the consequences of hinge-bending motions and does not (other than in the case of Alm/water) imply greater stability of the N-terminal segment of the molecule. Indeed, except for Alm/water, a similar picture would be obtained by superimposing the C-terminal segments of the molecule. Examination of such superimposed snapshots reinforces the impression of the similarity of the behavior of the peptide in the Alm/MeOH, Alm/POPC, and AlmH/POPC simulations. Clearly there is a similar degree of hinge-bending motion of the peptide backbone in all three simulations. The Alm/water simulation is rather different, showing conservation of the helix backbone conformation in the N-terminal half of the molecule comparable to that in the other three simulations, but revealing considerable conformational flexibility of the C-terminal half of the molecule. Thus whereas the motion in the three hydrophobic environments seems to be simply hinge-bending of two helical domains about a proline-induced kink, in water the C-terminal region adopts a flexible, essentially "random coil" conformation. Again, there does not appear to be any significant effect of protonation of the Glu^{18} residue on the behavior of the membrane-inserted Alm molecule.

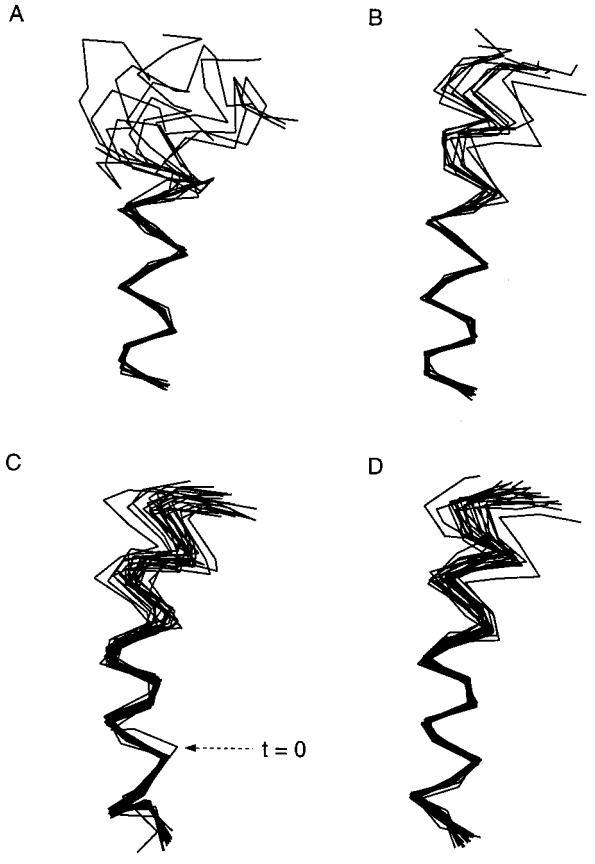

FIGURE 4 Cα traces, corresponding to structures saved every 100 ps, for (*A*) Alm/water, (*B*) Alm/MeOH, (*C*) Alm/POPC, and (*D*) AlmH/POPC. In each case the structures were superimposed by fitting their N-terminal helices (residues 1–11), and the N-termini are at the bottom of the diagram. Note the "jump" in structure for Alm/POPC around residues 3 and 4 shortly after $t = 0$ (highlighted by *arrow*).

The hinge-bending motions of Alm may be examined in more detail by combining essential dynamics (Amadei et al., 1993) with the DYNDOM analysis of Hayward and Berendsen (1998) to reveal the major components of the motions. For Alm/POPC this suggested that the motion could best be described as three rigid domains (residues 1–5, residues 6–10, and residues 11–20) moving relative to one another. For AlmH/POPC this is simplified to two rigid domains, namely residues 1–10 and residues 11–20. In the latter case, the angle of rotation between the two most extreme structures was 34°. Thus this more formal analysis of the intramolecular motions of Alm in three different simulations in explicit bilayer or bilayer-mimetic environments seems to confirm the picture arrived at in simple mean-field simulations of the Alm helix in a bilayer (Biggin et al., 1997).

It is of interest to examine the changes in the time-averaged molecular dipole of Alm between the Alm/water and e.g., Alm/POPC simulations. It has been suggested that voltage gating of Alm might be associated with a voltage-driven conformational change (e.g., coil $\rightarrow$ helix) of the C-terminal segment of the molecule (reviewed in, e.g., Sansom, 1993). Calculation of molecular dipoles for the Alm peptide backbone gives values of 55 ($\pm$1), 54 ($\pm$2), and 57 ($\pm$1) Debyes (1 Debye = 0.0209 e.nm) for Alm/MeOH, Alm/POPC, and AlmH/POPC, respectively. These values should be compared to an estimate (Sansom, 1991) of $\sim$63 Debyes for the dipole of the backbone of an idealized 20-residue α-helix. In contrast, the dipole for Alm/water averaged over the whole simulation is 47 ($\pm$4) Debyes. Furthermore, a plot of the backbone dipole versus time shows a transition at $\sim$300 ps (the same time as the major change in secondary structure; see next section). For t = 0–300 ps, the mean dipole is 52 ($\pm$4) Debye; for t = 300-1000 ps it is 45 ($\pm$2) Debye. Thus the greater disorder of the C-terminal segment of Alm in water leads to a small percentage loss in molecular dipole. Even if the coil $\rightarrow$ helix transition was coupled to a 100-mV drop across a bilayer, this would only yield an additional stabilization of $\sim$0.7 kJ/mol. This is likely to be insignificant compared to changes in hydrogen bonding energies and lipid/protein interactions associated with such a transition. Thus it seems unlikely that a voltage-driven coil $\rightarrow$ helix transition plays a crucial role in Alm channel gating.

Secondary structure

A more fine-grained description of the conformational dynamics of Alm in the three different environments is provided by analysis of the time-dependent secondary structure. Comparison of Alm/water and Alm/MeOH (Fig. 5, *A* and *B*) reveals a major difference. For Alm/MeOH the largely α-helical conformation of the peptide is maintained throughout the 1-ns duration of the simulation. There are occasional local deviations from α-helicity in the C-terminal half of the molecule. For Alm/water, there is loss of α-helicity at the C-terminus of the molecule starting at ~150 ps and reaching its maximum extent at ~300 ps. The N-terminal segment remains α-helical, whereas the C-terminal segment switches dynamically between bend, turn, and coil conformations. For example, over the final 100 ps of the simulation, residues 1–12 remain in an α-helical conformation, residues 13–15 fluctuate between bend and coil conformations, and residues 16–18 adopt a turn conformation.

This flexibility may be analyzed further by examination of trajectories for backbone Φ and ψ angles of individual residues (not shown). For the Alm/water simulation these reveal considerable fluctuations in backbone dihedrals, especially for residues Gly^{11}, Aib^{13}, Pro^{14}, Val^{15}, and Glu^{18}. Val^{15} in particular shows a major transition from the α- to the β-region of the Ramachandran plot at ~250 ps. For the Alm/MeOH simulation some fluctuations are seen for residues Gly^{11}, Leu^{12}, and Pro^{14}, which may be compared with the results of Gibbs et al. (1997) and Sessions et al. (1998), although the fluctuations are somewhat less long-lived in the current simulation (possibly reflecting differences in the force field). The average dihedral angles for each residue may be compared for Alm/water and Alm/MeOH (Fig. 6 *A*). Both simulations show greater deviation from the canonical

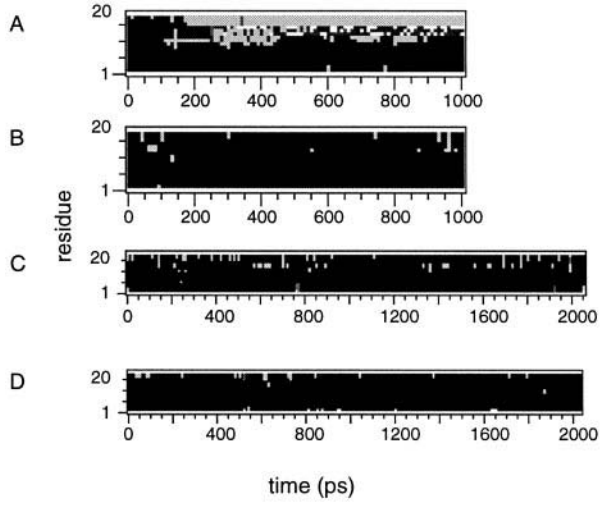

FIGURE 5 Secondary structure, as analyzed using DSSP (Kabsch and Sander, 1983), as a function of time for (*A*) Alm/water; (*B*) Alm/MeOH; (*C*) Alm/POPC; and (*D*) AlmH/POPC. Gray scale: black, α-helix; dark gray, bend; pale gray, turn; white, coil.

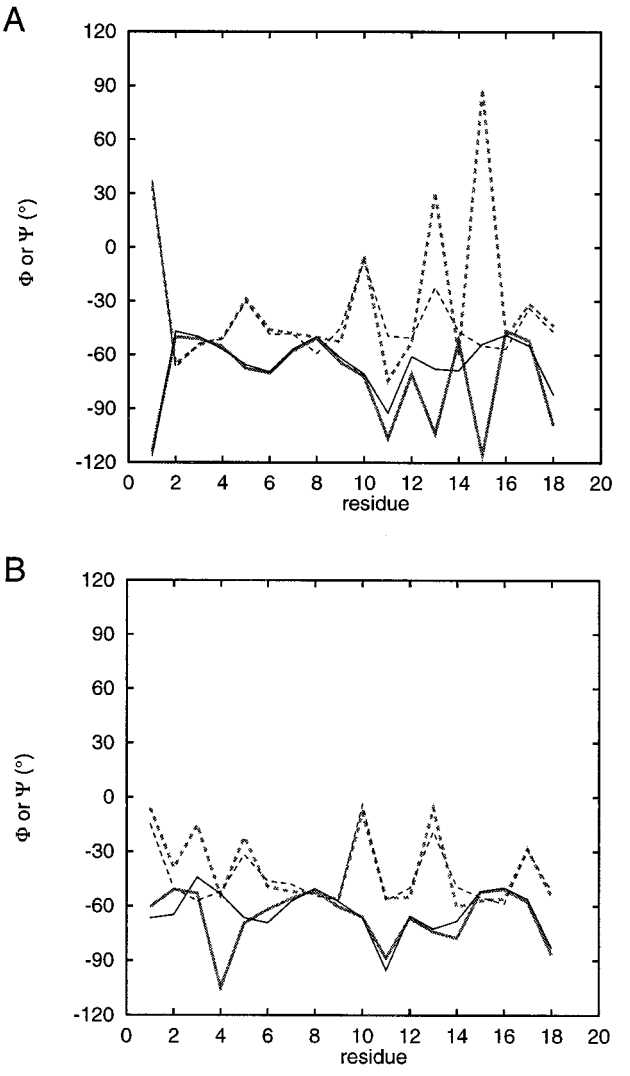

FIGURE 6 Time-averaged values of backbone Φ (*solid lines*) and ψ (*broken lines*) angles versus residue number. (*A*) Alm/water (*thick gray lines*) and Alm/MeOH (*thin black lines*). (*B*) Alm/POPC (*thick gray lines*) and AlmH/POPC (*thin black lines*).

α-helical values for the C-terminal segment than for the N-terminal segment, but these deviations are much more marked for the Alm/water simulation. The values for Alm/MeOH compare well with those determined in the x-ray (Fox and Richards, 1982) structure; the differences are at the termini and in the Gly-X-X-Pro "hinge" region.

Turning to Alm/POPC and AlmH/POPC, the diagrams of secondary structure versus time (Fig. 5, *C* and *D*) reveal that the α-helical conformation of Alm is largely preserved throughout both 2-ns simulations, with only occasional and brief fluctuations leading to a few residues of, e.g., turn conformation. The fluctuations seem to be slightly more marked for Alm/POPC than for AlmH/POPC, although it is difficult to decide whether this difference is statistically significant. It may reflect a higher frequency of Alm/water H-bonding for the form with the ionized Glu side chain (see below). Analysis of the average values of backbone dihe-

drals versus residue (Fig. 6 *B*) shows no major differences between Alm/POPC and AlmH/POPC (other than for residues 3 and 4 in Alm/POPC; see below) or between these two simulations and Alm/MeOH. Analysis of the backbone dihedrals as functions of time reveals the reason for the difference in the Cα RMSD plots for Alm/POPC and AlmH/POPC (see above). In AlmH/POPC the backbone dihedrals show small fluctuations for Gly^{11} and Leu^{12}, i.e., much the same as for Alm/MeOH. Alm/POPC shows similar fluctuations for Gly^{11} and Leu^{12}. However, in addition, Alm/POPC shows a jump in the values of ψ for Aib^3 and of Φ for Ala^4 at $t \approx 100$ ps away from standard α-helical values (i.e., $\psi_3 \approx -40°$, $\Phi_4 \approx -60°$) toward a more distorted conformation (i.e., $\psi_3 \approx -16°$, $\Phi_4 \approx -105°$). This explains the initial rise in Cα RMSD over the first 100 ps. There is a brief transition back to ($\psi_3 \approx -40°$, $\Phi_4 \approx 60°$) at $t \approx 800$ ps, but this lasts for only ~30 ps before the more distorted conformation is resumed. Other than this local distortion in the N-terminal segment, the helical conformation is retained in Alm/POPC, and the helix conformation is the same as that in AlmH/POPC and Alm/MeOH. So overall, Alm retains a largely α-helical conformation when inserted into a lipid bilayer, and this is similar to its behavior in a bilayer-mimetic environment.

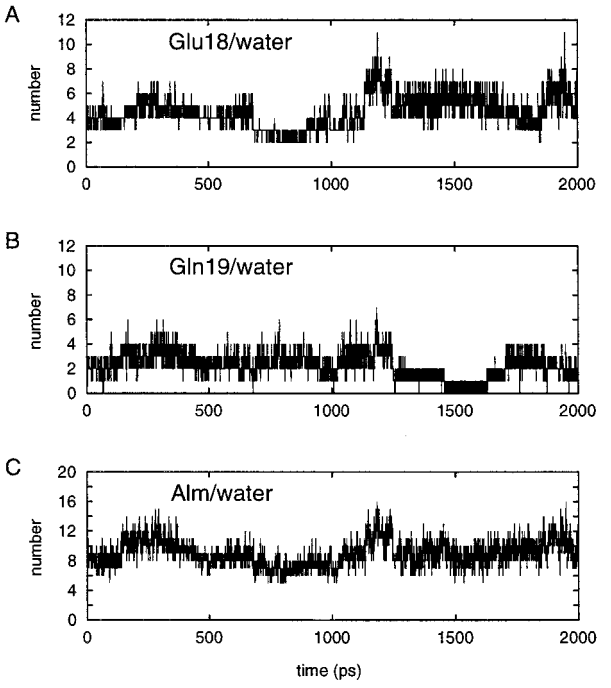

FIGURE 7 Analysis of H-bonds in the Alm/POPC simulations. (*A*) Glu^{18}/water. (*B*) Gln^{19}/water. (*C*) Alm (all atoms)/water. In each case the number of H-bonds is shown as a function of time.

The C-terminal "anchor"

As discussed above, an intriguing property of Alm revealed by electrophysiological studies (reviewed by Sansom, 1993) is that it is much easier for the N-terminus of the helix to insert into a lipid bilayer than for the C-terminus. A series of early experiments (Hall et al., 1984) showed how this aspect of the peptide's function changed as its structure was changed. Thus, for native Alm, the C-terminus appears to act as a sort of "anchor" at the bilayer surface. We were interested in seeing whether MD simulations of bilayer-inserted Alm would suggest the molecular basis of this C-terminal anchor.

One may approach the nature of the C-terminal anchor in terms of the energetics of the interactions of Alm with lipid molecules and with water molecules when inserted into a POPC bilayer. From these data (not shown) it is evident that the Alm helix forms significant electrostatic interactions with its environment (both lipid and water), even when inserted into a lipid bilayer. We may examine this in more detail by counting the number of H-bonds made by different residues of the Alm molecule. Such analysis is presented (for Alm/POPC) in Fig. 7. The Glu^{18} residue forms on average approximately five H-bonds to water, even when Alm is inserted into the bilayer. The Gln^{19} residue forms on average approximately two H-bonds to water. The total number of H-bonds to water averages ~10. Thus ~70% of the H-bonds to water are formed by the two C-terminal residues. Significantly, these two residues (Glu^{18}-Gln^{19}) are conserved (although the Glu may be a Gln) in a wide range of peptaibols (see http://www.cryst.bbk.ac.uk/peptaibol/). Indeed, the C-terminal sequence motif for nearly all peptaibols is Glu/Gln-Gln-X, where X = Phe, Leu, Ile, Trp (in decreasing frequency of occurrence). There are also H-bonds to the lipid from the C-terminus of Alm. Two H-bonds to lipid persist throughout the simulation, one from the -NH_2 of the side chain of Gln^{19} to the ester oxygen of a lipid and the other from the terminal phenylalaninol -OH, again to an ester oxygen. Similar analysis for AlmH also reveals substantial H-bonding of the C-terminus of the Alm molecule to water in the interfacial region, although protonation reduces this for the Glu^{18} side chains. AlmH also shows a persistent H-bond from the -NH_2 of the side chain of Gln^{19} to the ester oxygen of a lipid and fluctuating H-bonds from the Glu^{18} side chain and the terminal -OH to lipid.

A clear picture of the role of the C-terminal side chains in H-bonding to water in the interfacial region may be obtained from snapshots of Alm/water interactions (Fig. 8). In a pure bilayer simulation the water rarely penetrates the bilayer beyond the carbonyl groups of the fatty acyl chains (Marrink and Berendsen, 1994; Tieleman et al., 1997). Examination of the Alm/POPC simulation reveals that a water is persistently H-bonded to the acidic side chain of Glu^{18}, "pulling" that water into the bilayer beyond the fatty acyl carbonyl "limit." This correlates with the quantitative analysis of Alm/water H-bonding provided above. Together these two analyses suggest that the pair of polar side chains at positions 18 and 19 constitute the basis of the C-terminal anchor. No such marked Alm/water interactions are seen at the N-terminus of the molecule. Thus, on the basis of the

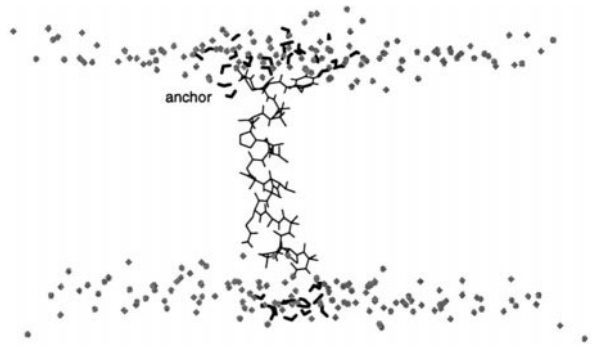

FIGURE 8 Snapshot (at $t = 2$ ns) of the Alm/POPC simulation illustrating the Alm/water interactions. The Alm molecule is shown by thin black bonds, those waters within 0.6 nm of the peptide by thick black bonds, and the carbonyl oxygens of the POPC molecules by gray dots. The water molecules close to the C-terminal anchor residues are labeled.

MD simulations of Alm in POPC, one is able to suggest a molecular explanation of the asymmetrical insertion properties of the Alm helix.

DISCUSSION

The simulations presented above are, to the best of our knowledge, the first that investigate Alm/bilayer interactions using an all-atom, as opposed to mean-field (Biggin et al., 1997), model of the membrane. The simulations of Alm/water and Alm/MeOH complement previous simulations of Alm in methanol (Gibbs et al., 1997). However, one should be aware of the limitations of the simulation technique employed. The first is the length of the simulations. Although 1–2 ns is a reasonable duration by current standards, one remains uncertain of whether significant changes in Alm/bilayer interactions would occur if the simulation lengths were extended. However, the similar results from the Alm/POPC and AlmH/POPC simulations lend some hope that 2-ns simulations have captured the essence of the peptide/bilayer interactions, at least on a shorter time scale. A second limitation is the relatively simple treatment of electrostatics in the current simulations. This protocol has been shown to give reasonable agreement with experimental results for pure bilayer simulations (Tieleman et al., 1997) and to yield stable simulations for the porin OmpF in a palmitoyloleoyl phosphatidylethanolamine bilayer (Tieleman and Berendsen, 1998). However, a number of studies have been concerned with the effects of different treatments of long-range electrostatic interactions (Tieleman et al., 1997; Tobias et al., 1997), and this is clearly an area that will merit further study. The third concern is the use of a structure of an Alm monomer generated by restrained in vacuo MD as the starting point for the simulations. What would happen if, e.g., one of three monomers of the crystallographic asymmetrical unit (Fox and Richards, 1982) or, e.g., a model of Alm in an exactly α-helical conformation (Gibbs et al., 1997) was used as the starting point? One may draw some comfort from the observation that in vacuo restrained MD simulations of Alm monomers starting from highly idealized α-helices yielded structures that were essentially the same as those in the crystal (Biggin et al., 1997). This suggests that the model-building procedure generates a stable conformation of Alm when in a nonaqueous environment. It should be noted that Alm was crystallized from a hydrophobic solvent environment.

The results of these simulations are of particular interest in the context of the stability of Alm in different environments and the light this casts on the early stages of the mechanism of channel formation by this much-studied peptide. It is evident that Alm in water does not adopt a single conformation; rather, like many peptides, it is quite flexible. This is despite the presence of the helicogenic amino acid Aib in the Alm sequence. The current simulations suggest that the C-terminus of the helix is less stable than the N-terminus. However, it must be remembered that this simulation was started from a model of Alm in a helical conformation and was only run for 1 ns. Clearly the simulation had not reached an equilibrium, and further unfolding of the molecule might have taken place if the simulation was significantly extended. Perhaps the safest conclusion is to state that the C-terminal segment of the Alm helix unfolds first when the peptide is in an aqueous environment. This should be compared with the NMR amide exchange data of Dempsey and Handcock (1996), who concluded that alamethicin in water is only partly structured (although their results suggested greater stability of the C-terminal segment of the helix rather than the N-terminal helix). Thus, before it associates with a membrane, the Alm helix is relatively unstable.

Once the Alm helix has inserted in a bilayer it is quite stable and undergoes relatively limited hinge-bending motions. This behavior is very similar to that of Alm in membrane-mimetic environments. For example, by comparing NMR amide exchange data with MD simulations, Gibbs et al. (1997) concluded that the Alm helix was largely stable in MeOH but exhibited hinge-bending around residues 10–13. Similarly, Franklin et al. (1994) used NMR to examine the conformation of Alm bound to sodium dodecyl sulfate (SDS) micelles. Their results suggested structural fluctuations of residues 10–12, with a largely helical structure retained in both the N- and C-terminal segments flanking this region. Furthermore, Spyracopoulos et al. (1996) have suggested that the peptide backbone of Alm is intermediate in flexibility between the core of a folded, globular protein and the disordered regions of the latter, although they saw some differences in dynamics between Alm in MeOH and Alm bound to SDS micelles. Thus the motions of membrane-inserted Alm in our simulations are in general agreement with the available experimental data for a membrane-mimetic environment. Once inserted into a bilayer, the Alm helix has a reasonable propensity to remain there, with the C-terminal polar residues providing an anchor to the bilayer surface. This suggests that, in terms of channel formation, part of the voltage-driven process may be to simply increase the ratio of inserted to surface-bound Alm helices. As has

been shown by, e.g., Huang and Wu (1991), Alm helices can (albeit at relatively high peptide-to-lipid ratios) insert into a bilayer in the absence of a transbilayer voltage. It is also of interest that recent measurements of the transmembrane migration rate of Alm reveal it to be slower than expected, an observation that has been interpreted in terms of a barrier to transport at the C-terminus due to H-bonding to lipid and/or water (Jayasinghe et al., 1998).

The results of these simulations of Alm inserted into a lipid bilayer may also be of more general significance for integral membrane proteins. As has been noted by, e.g., Brandl and Deber (1986), although rare within helices in soluble proteins, proline residues occur with a relatively high frequency in (predicted) TM helices of integral membrane proteins. The structural role of prolines in integral membrane proteins has been investigated by, e.g., von Heijne (1991). Alm inserted into a POPC bilayer may serve as a model for these more complex structures. From the simulations discussed above, it is clear that an intrahelical proline may act as a molecular "hinge" when in a bilayer environment. Of course, in most membrane proteins the proline will not be in an isolated TM helix, but in a TM helix within a bundle of such helices. It would be of some interest to see whether helix hinge-bending motions still occur within such helix bundles, and if so, whether such motions might have any functional role. In the latter context, we note that a molecular hinge within a TM helix has been suggested to play a role in gating of the nicotinic acetylcholine receptor ion channel (Sankararamakrishnan et al., 1996; Unwin, 1995), although in this case the hinge is not associated with a proline residue.

The current studies of Alm inserted into a lipid bilayer may be compared with other recent simulations of TM α-helices inserted into lipid bilayers. Three detailed simulation studies have confirmed the stability of TM helices when simulated in a phospholipid bilayer (Shen et al., 1997, #785; Woolf, 1997, #940; Belohorcova et al., 1997). In particular, Shen et al. (1997) have suggested, on the basis of simulations of an Ala_{32} α-helix spanning a dimyristoylphosphatidylcholine (DMPC) bilayer, that some degree of bending in the center of a TM helix may be required to accommodate relative motions of the two leaflets of the bilayer. This is an intriguing suggestion in the context of the hinge-bending motion of Alm in a bilayer. Perhaps Alm is designed to exactly match the dynamics of its transbilayer environment. Enhanced TM helix mobility due to proline residues was also observed in MD simulations of individual helices from bacteriorhodopsin in a DMPC bilayer (Woolf, 1997). Belohorcova et al. (1997), studying a simplified model of a TM helix ($K_2GL_{16}K_2A$), showed that the lysine residues at either end of the helix interacted strongly with waters in the interfacial region, in a manner similar to that of the residues of the C-terminal anchor of Alm.

In summary, the simulations presented in this paper provide the first detailed MD study of an Alm helix inserted into a phospholipid bilayer. There are three major directions in which this work must be extended if one is to understand the channel-forming properties of Alm at atomic resolution. The first is to extend such simulations to models of Alm helix bundles inserted into a lipid bilayer. This is the subject of a forthcoming paper (Tieleman, Berendsen and Sansom, manuscript in preparation). The second extension is to consider the "missing" early step in channel formation by Alm, namely to simulate the interactions of an Alm helix with the bilayer surface before insertion. Preliminary studies (Sansom et al., unpublished data) suggest that interactions with the surface help to stabilize Alm's helical conformation relative to the peptide in aqueous solution. The third, and perhaps more difficult, extension will be to simulate V-dependent insertion of an Alm helix. This has been attempted with a simple mean-field model (Biggin et al., 1997), and recent theoretical studies (Roux, 1997) have suggested how a transbilayer voltage might be more rigorously treated in simulations. However, it remains to conduct all-atom simulations of voltage-induced insertion of Alm.

Work in the laboratory of MSPS is supported by the Wellcome Trust. DPT was supported in part by the European Union under contract CT94-0124.

REFERENCES

Åkerfeldt, K. S., J. D. Lear, Z. R. Wasserman, L. A. Chung, and W. F. DeGrado. 1993. Synthetic peptides as models for ion channel proteins. *Acc. Chem. Res.* 26:191–197.

Amadei, A., A. B. M. Linssen, and H. J. C. Berendsen. 1993. Essential dynamics of proteins. *Proteins Struct. Funct. Genet.* 17:412–425.

Barranger-Mathys, M., and D. S. Cafiso. 1996. Membrane structure of voltage-gated channel-forming peptides by site-directed spin-labeling. *Biochemistry.* 35:498–505.

Belohorcova, K., J. H. Davis, T. B. Woolf, and B. Roux. 1997. Structure and dynamics of an amphiphilic peptide in a lipid bilayer: a molecular dynamics study. *Biophys. J.* 73:3039–3055.

Berendsen, H. J. C., J. P. M. Postma, W. F. van Gunsteren, A. DiNola, and J. R. Haak. 1984. Molecular dynamics with coupling to an external bath. *J. Chem. Phys.* 81:3684–3690.

Berendsen, H. J. C., D. van der Spoel, and R. van Drunen. 1995. GROMACS: a message-passing parallel molecular dynamics implementation. *Comp. Phys. Comm.* 95:43–56.

Berger, O., O. Edholm, and F. Jahnig. 1997. Molecular dynamics simulations of a fluid bilayer of dipalmitoylphosphatidycholine at full hydration, constant pressure and constant temperature. *Biophys. J.* 72: 2002–2013.

Biggin, P., J. Breed, H. S. Son, and M. S. P. Sansom. 1997. Simulation studies of alamethicin-bilayer interactions. *Biophys. J.* 72:627–636.

Boyd, D., C. Schierle, and J. Beckwith. 1998. How many membrane proteins are there? *Protein Sci.* 7:201–205.

Brandl, C. J., and C. M. Deber. 1986. Hypothesis about the function of membrane-buried proline residues in transport proteins. *Proc. Natl. Acad. Sci. USA.* 83:917–921.

Cafiso, D. S. 1994. Alamethicin—a peptide model for voltage gating and protein membrane interactions. *Annu. Rev. Biophys. Biomol. Struct.* 23:141–165.

Dempsey, C. E. 1995. Hydrogen-bond stabilities in the isolated alamethicin helix—pH-dependent amide exchange measurements in methanol. *J. Am. Chem. Soc.* 117:7526–7534.

Dempsey, C. E., and L. J. Handcock. 1996. Hydrogen-bond stabilities in membrane-reconstituted alamethicin from amide-resolved hydrogen-exchange measurements. *Biophys. J.* 70:1777–1788.

Esposito, G., J. A. Carver, J. Boyd, and I. D. Campbell. 1987. High resolution ^{1}H NMR study of the solution structure of alamethicin. *Biochemistry.* 26:1043–1050.

Fox, R. O., and F. M. Richards. 1982. A voltage-gated ion channel model inferred from the crystal structure of alamethicin at 1.5 Å resolution. *Nature.* 300:325–330.

Franklin, J. C., J. F. Ellena, S. Jayasinghe, L. P. Kelsh, and D. S. Cafiso. 1994. Structure of micelle-associated alamethicin from ^{1}H-NMR—evidence for conformational heterogeneity in a voltage-gated peptide. *Biochemistry.* 33:4036–4045.

Fraternali, F. 1990. Restrained and unrestrained molecular dynamics simulations in the NVT ensemble of alamethicin. *Biopolymers.* 30: 1083–1099.

Gazit, E., I. R. Miller, P. C. Biggin, M. S. P. Sansom, and Y. Shai. 1996. Structure and orientation of the mammalian antibacterial peptide cecropin P1 within phospholipid membranes. *J. Mol. Biol.* 258: 860–870.

Gibbs, N., R. B. Sessions, P. B. Williams, and C. E. Dempsey. 1997. Helix bending in alamethicin: molecular dynamics simulations and amide hydrogen exchange in methanol. *Biophys. J.* 72:2490–2495.

Hall, J. E., I. Vodyanoy, T. M. Balasubramanian, and G. R. Marshall. 1984. Alamethicin: a rich model for channel behaviour. *Biophys. J.* 45: 233–247.

Hayward, S., and H. J. C. Berendsen. 1998. Systematic analysis of domain motions in proteins from conformational change: new results on citrate synthase and T4 lysozyme. *Proteins Struct. Funct. Genet.* 30:144–154.

Hermans, J., H. J. C. Berendsen, W. F. van Gunsteren, and J. P. M. Postma. 1984. A consistent empirical potential for water-protein interactions. *Biopolymers.* 23:1513–1518.

Huang, H. W., and Y. Wu. 1991. Lipid-alamethicin interactions influence alamethicin orientation. *Biophys. J.* 60:1079–1087.

Jakobsson, E. 1997. Computer simulation studies of biological membranes: progress, promise and pitfalls. *Trends Biochem. Sci.* 22:339–344.

Jayasinghe, S., M. Barranger-Mathys, J. F. Ellena, C. Franklin, and D. S. Cafiso. 1998. Structural features that modulate the transmembrane migration of a hydrophobic peptide in lipid vesicles. *Biophys. J.* 74: 3023–3030.

Kabsch, W., and C. Sander. 1983. Dictionary of protein secondary structure: pattern recognition of hydrogen-bonded and geometrical features. *Biopolymers.* 22:2577–2637.

Kraulis, P. J. 1991. MOLSCRIPT: a program to produce both detailed and schematic plots of protein structures. *J. Appl. Crystallogr.* 24:946–950.

Lear, J. D., Z. R. Wasserman, and W. F. DeGrado. 1988. Synthetic amphiphilic peptide models for protein ion channels. *Science.* 240: 1177–1181.

Lear, J. D., Z. R. Wasserman, and W. F. DeGrado. 1994. Use of synthetic peptides for the study of membrane protein structure. *In* Membrane Protein Structure: Experimental Approaches. Oxford University Press, Oxford.

Marrink, S. J., and H. J. C. Berendsen. 1994. Simulation of water transport through a lipid membrane. *J. Phys. Chem.* 98:4155–4168.

Marrink, S. J., O. Berger, D. P. Tieleman, and F. Jahnig. 1998. Adhesion forces of lipids in a phospholipid membrane studied by molecular dynamics simulations. *Biophys. J.* 74:931–943.

Merz, K. M. 1997. Molecular dynamics simulations of lipid bilayers. *Curr. Opin. Struct. Biol.* 7:511–517.

Merz, K. M., and B. Roux. 1996. Biological Membranes: A Molecular Perspective from Computation and Experiment. Birkhäuser, Boston.

North, C. L., M. Barranger-Mathys, and D. S. Cafiso. 1995. Membrane orientation of the N-terminal segment of alamethicin determined by solid-state ^{15}N NMR. *Biophys. J.* 69:2392–2397.

Polinsky, A., M. Goodman, K. A. Williams, and C. M. Deber. 1992. Minimum energy conformations of proline-containing helices. *Biopolymers.* 32:399–406.

Roux, B. 1997. Influence of the membrane potential on the free energy of an intrinsic protein. *Biophys. J.* 73:2980–2989.

Sankararamakrishnan, R., C. Adcock, and M. S. P. Sansom. 1996. The pore domain of the nicotinic acetylcholine receptor: molecular modelling and electrostatics. *Biophys. J.* 71:1659–1671.

Sankararamakrishnan, R., and S. Vishveshwara. 1992. Geometry of proline-containing alpha-helices in proteins. *Int. J. Pept. Protein Res.* 39: 356–363.

Sansom, M. S. P. 1991. The biophysics of peptide models of ion channels. *Prog. Biophys. Mol. Biol.* 55:139–236.

Sansom, M. S. P. 1992. Proline residues in transmembrane helices of channel and transport proteins: a molecular modelling study. *Protein Eng.* 5:53–60.

Sansom, M. S. P. 1993. Structure and function of channel-forming peptaibols. *Q. Rev. Biophys.* 26:365–421.

Sessions, R. B., N. Gibbs, and C. E. Dempsey. 1998. Hydogen bonding in helical polypeptides from molecular dynamics simulations and amide exchange analysis: alamethicin and melittin in methanol. *Biophys. J.* 74:138–152.

Shen, L., D. Bassolino, and T. Stouch. 1997. Transmembrane helix structure, dynamics, and interactions: multi-nanosecond molecular dynamics simulations. *Biophys. J.* 73:3–20.

Spyracopoulos, L., A. A. Yee, and J. D. J. O'Neil. 1996. Backbone dynamics of an alamethicin in methanol and aqueous detergen solution determined by heteronuclear H^{1}-N^{15} NMR spectroscopy. *J. Biomol. NMR.* 7:283–294.

Tieleman, D. P., and H. J. C. Berendsen. 1996. Molecular dynamics simulations of a fully hydrated dipalmitoylphosphatidycholine bilayer with different macroscopic boundary conditions and parameters. *J. Chem. Phys.* 105:4871–4880.

Tieleman, D. P., and H. J. C. Berendsen. 1998. A molecular dynamics study of the pores formed by *E. coli* OmpF porin in a fully hydrated POPE bilayer. *Biophys. J.* 74:2786–2801.

Tieleman, D. P., S. J. Marrink, and H. J. C. Berendsen. 1997. A computer perspective of membranes: molecular dynamics studies of lipid bilayer systems. *Biochim. Biophys. Acta.* 1331:235–270.

Tobias, D. J., K. C. Tu, and M. L. Klein. 1997. Atomic-scale molecular dynamics simulations of lipid membranes. *Curr. Opin. Colloid Interface Sci.* 2:15–26.

Unwin, N. 1995. Acetylcholine receptor channel imaged in the open state. *Nature.* 373:37–43.

van Gunsteren, W. F., P. Kruger, S. R. Billeter, A. E. Mark, A. A. Eising, W. R. P. Scott, P. H. Huneberger, and I. G. Tironi. 1996. Biomolecular Simulation: The GROMOS96 Manual and User Guide. Biomos & Hochschulverlag AG an der ETH Zurich, Groningen and Zurich.

Vogel, H. 1987. Comparison of the conformation and orientation of alamethicin and melittin in lipid membranes. *Biochemistry.* 26:4562–4572.

von Heijne, G. 1991. Proline kinks in transmembrane α-helices. *J. Mol. Biol.* 499–503.

Wallin, E., and G. von Heijne. 1998. Genome-wide analysis of integral membrane proteins from eubacterial, archean, and eukaryotic organisms. *Protein Sci.* 7:1029–1038.

Woolf, T. B. 1997. Molecular dynamics of individual α-helices of bacteriorhodopsin in dimyristoyl phosphatidylcholine. I. Structure and dynamics. *Biophys. J.* 73:2376–2392.

Woolfson, D. N., R. J. Mortishire-Smith, and D. H. Williams. 1991. Conserved positioning of proline residues in membrane-spanning helices of ion-channel proteins. *Biochem. Biophys. Res. Commun.* 175:733–737.

Woolley, G. A., and B. A. Wallace. 1992. Model ion channels: gramicidin and alamethicin. *J. Membr. Biol.* 129:109–136.

Yun, R. H., A. Anderson, and J. Hermans. 1992. Proline in α-helix: stability and conformation studied by dynamics simulation. *Proteins Struct. Funct. Genet.* 10:219–228.